the FEBS Journal

NMR study of complexes between low molecular mass inhibitors and the West Nile virus NS2B–NS3 protease

Xun-Cheng Su[1], Kiyoshi Ozawa[1], Hiromasa Yagi[1], Siew P. Lim[2], Daying Wen[2], Dariusz Ekonomiuk[3], Danzhi Huang[3], Thomas H. Keller[2], Sebastian Sonntag[2], Amedeo Caflisch[3], Subhash G. Vasudevan[2,*] and Gottfried Otting[1]

1 Research School of Chemistry, Australian National University, Canberra, Australia
2 Novartis Institute for Tropical Diseases, Singapore
3 Department of Biochemistry, University of Zürich, Switzerland

Keywords
drug development; inhibitors; NMR spectroscopy; NS2B–NS3 protease; West Nile virus

Correspondence
G. Otting, Research School of Chemistry, Australian National University, Canberra, ACT 0200, Australia
Fax: +61 2 612 50750
Tel: +61 2 612 56507
E-mail: go@rsc.anu.edu.au

***Present address**
Program in Emerging Infectious Diseases, Duke-NUS Graduate Medical School, Singapore

Note
Xun-Cheng Su and Kiyoshi Ozawa contributed equally to this work

(Received 28 February 2009, revised 9 April 2009, accepted 4 June 2009)

doi:10.1111/j.1742-4658.2009.07132.x

The two-component NS2B–NS3 protease of West Nile virus is essential for its replication and presents an attractive target for drug development. Here, we describe protocols for the high-yield expression of stable isotope-labelled samples *in vivo* and *in vitro*. We also describe the use of NMR spectroscopy to determine the binding mode of new low molecular mass inhibitors of the West Nile virus NS2B–NS3 protease which were discovered using high-throughput *in vitro* screening. Binding to the substrate-binding sites S1 and S3 is confirmed by intermolecular NOEs and comparison with the binding mode of a previously identified low molecular mass inhibitor. Our results show that all these inhibitors act by occupying the substrate-binding site of the protease rather than by an allosteric mechanism. In addition, the NS2B polypeptide chain was found to be positioned near the substrate-binding site, as observed previously in crystal structures of the protease in complex with peptide inhibitors or bovine pancreatic trypsin inhibitor. This indicates that the new low molecular mass compounds, although inhibiting the protease, also promote the proteolytically active conformation of NS2B, which is very different from the crystal structure of the protein without inhibitor.

Introduction

West Nile virus (WNV) encephalitis is a mosquito-borne disease that infects mainly birds, but also animals and humans. It occurs in Africa, Europe and Asia and, since 1999, has also been spreading in North America, causing several thousand cases per year, with a fatality rate of ~5%, as reported by the US Department of Health [1].

WNV is a member of the flavivirus genus along with yellow fever virus, dengue virus and Japanese encephalitis virus, all of which cause human diseases. There is no vaccine or specific antiviral therapy currently in existence for WNV encephalitis in humans. During infection, the flavivirus RNA genome is translated into a polyprotein, which is cleaved into several

Abbreviations
BPTI, bovine pancreatic trypsin inhibitor; Bz-nKRR-H, benzoyl-norleucine-lysine-arginine-arginine-aldehyde; HTS, high-throughput screen; WNV, West Nile virus.

components. Nonstructural protein 3 (NS3) is responsible for proteolysis of the polyprotein through its serine protease N-terminal domain (NS3pro), in conjunction with a segment of ~40 residues from the NS2B protein acting as a co-factor. NS3 is essential for viral replication and therefore presents an attractive drug target. The C-terminal two-thirds of NS3, which contain a nucleotide triphosphatase, an RNA triphosphatase and a helicase, have been shown to have little influence on protease activity [2], although the 3D structure of the full-length dengue virus DENV-4 NS3 protease–helicase suggests that the protease domain assists the binding of nucleotides to the helicase and may also participate in RNA unwinding [3].

Crystal structures of WNV NS2B–NS3pro have been reported in the absence of inhibitor [4] and in the presence of peptide inhibitors [5,6] or bovine pancreatic trypsin inhibitor (BPTI) [4]. In the absence of inhibitor, the structure shows the β-hairpin of NS2B positioned far (almost 40 Å) from the active site. Because the C-terminal residues of NS2B are not only essential for full catalytic activity of WNV NS2B–NS3pro [7,8], but are also found near the active site in the structures with peptide inhibitors and BPTI, the proteolytically most active conformations are thought to be represented by the structures observed with inhibitors rather than the one without inhibitor. The function of the protease is preserved in a 28 kDa construct in which NS2B and NS3pro are fused via a Gly_4–Ser–Gly_4 linker (Fig. 2) [2,9].

A number of low molecular mass nonpeptidic inhibitors have been generated in hit-to-lead activities following a high-throughput screen (HTS) directed against dengue virus NS2B–NS3 protease (C. Bodenreider *et al.*, manuscript in preparation). Because of the high sequence homology between dengue virus and WNV, many of the compounds found to inhibit the dengue virus protease also inhibited WNV protease, albeit with different affinities (C. Bodenreider *et al.*, manuscript in preparation). Figure 1 shows three of the inhibitors found. Compounds **1** and **2** originated from the HTS, whereas compound **3** was discovered using the crystal structure of WNV NS2B–NS3pro with bound tetrapeptide [5] in an *in silico* screening approach [10]. Compounds **1** and **2** showed inhibition constants in the low micromolar range, but no related compounds could be found with inhibition constants below 1 μM (C. Bodenreider *et al.*, manuscript in preparation).

The results of two other published HTS efforts confirmed that discovery of high-affinity inhibitors for WNV NS2B–NS3pro is nontrivial. In one study, competitive inhibitors with an inhibition constant of

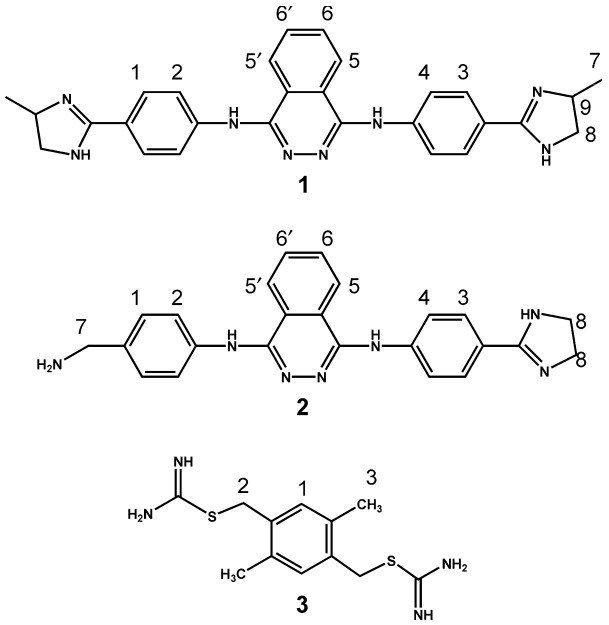

Fig. 1. Synthetic inhibitors **1–3** of WNV NS2B–NS3pro studied. Individual atoms are numbered as reference for NMR resonance assignments.

~3 μM were found and their binding to WNV NS2B–NS3pro modelled [11]. In another, noncompetitive inhibitors with IC_{50} values of ~0.1 μM were found, but these were prone to hydrolysis with deactivation half-lives of 1–2 h. The latter are thought to bind to NS3pro, displacing the C-terminal β-hairpin of NS2B from NS3pro [12]. HTS campaigns against the WNV replicon, in which the target protein is unknown, also failed to discover nonpeptidic inhibitors with inhibitory activities much below 1 μM [13,14], with an EC_{50} value of 0.85 μM being reported for the most active compound [15].

In order to improve our understanding of the action of compounds **1–3** against WNV NS2B–NS3pro, structural information about their binding modes must be obtained. Despite many efforts, however, no crystal structure of the protease could be determined in complex with compounds **1–3** or any other low molecular mass inhibitor. In view of the ability of NS2B to undergo a large structural change between proteolytically deactivated and fully active states, as observed in crystal structures [4,5], competitive inhibition may conceivably be achieved by binding to an allosteric site rather than to the active site. We therefore turned to solution NMR spectroscopy to identify the binding sites of **1–3** to WNV NS2B–NS3pro.

We have previously described a model of **3** bound to WNV NS2B–NS3pro, obtained by automatic computational docking, which is in agreement with the

intermolecular NOEs reported here [10]. Ekonomiuk *et al*. [10] also presented the dissociation constant of **3** measured by NMR and, as additional proof for binding of **3** to the substrate-binding site, demonstrated changes in cross-peak positions for residues lining the substrate-binding site, without discussing the complete resonance assignment.

In the following, we report protocols for the expression of isotope-labelled WNV NS2B–NS3pro in high yields in *Escherichia coli in vivo* and by cell-free synthesis, the first virtually complete assignments of the ^{15}N-HSQC spectrum, structure analysis of WNV NS2B–NS3pro with bound inhibitor, and identification of intermolecular NOEs between the inhibitors and the protease.

Results

Sample preparation

The original construct of NS2B–NS3pro (construct 1, Fig. 2) was toxic to *E. coli*, leading to cell lysis on plates prepared with rich media as well as in large-scale preparations. Improved protein yields were obtained by a modified protocol, where *E. coli* colonies grown on M9 media plates were selected prior to large-scale expression. In this way, 9.3 mg of purified uniformly ^{15}N/^{13}C-labelled protein were obtained per litre of a ^{15}N/^{13}C-labelled rich medium (induction by isopropyl β-D-thiogalactoside), whereas an autoinduction protocol [16] yielded as much as 59 mg of purified ^{15}N-labelled protein per litre of cell culture (Materials and methods).

Construct 1 equally produced hardly any protein in our cell-free protein synthesis system [17,18]. This problem was overcome by construct 2 which starts with the first six codons from T7 gene 10 and which expresses well in cell-free systems. A clone in a high-copy number T7 plasmid [19] facilitated the preparation of large quantities of DNA required for the cell-free synthesis. Typical yields were close to 1 mg of purified protein per mL of cell-free reaction mixture. Although acceptable ^{15}N-HSQC spectra could be recorded without purification of the protein [20,21], complex formation with the inhibitors required purified protein because compounds **1** and **2** also bound to components of the cell-free mixture.

The NS2B–NS3pro construct 1 in Fig. 2 was susceptible to gradual self-cleavage by the protease at two sites, following the first glycine in the linker after Lys96^{NS2B} and Lys15^{NS3} (Fig. 2) [5,22], resulting in release of the intermittent peptide from the protein. Because variable extents of cleavage led to sample heterogeneity, later work employed the mutant Lys96^{NS2B} → Ala (construct 3) which prevented cleavage at either site [23]. The K96A mutant turned out to be much less toxic to *E. coli*, producing high yields even when overexpression was induced by isopropyl β-D-thiogalactoside. The K96A mutant retained full proteolytic activity in the assay used (C. Bodenreider *et al*., manuscript in preparation) to measure the inhibition constant of different ligands (data not shown).

Inhibitor binding monitored by NMR spectroscopy

In the absence of inhibitors, assignment of the NMR resonances for WNV NS2B–NS3pro was difficult because many signals were broadened beyond detection and the spectral resolution was poor (Fig. 3A). Over 100 different compounds that had been suggested by high-throughput docking calculations with a large library of molecules [10] or had appeared as hits in the *in vitro* high-throughput screens were tested for binding to WNV NS2B–NS3pro by NMR spectroscopy using ^{15}N-labelled protein. 1D ^{1}N NMR spectra were used to assess any line broadening experienced by the low molecular mass compounds and ^{15}N-HSQC spectra were recorded to detect responses in the protein. Most of the compounds showed broad lines in the presence of protein without noticeably changing the ^{15}N-HSQC spectrum. This situation was interpreted as nonspecific binding. Other compounds were barely soluble in water. Compounds **1** and **2**, however, improved the ^{15}N-HSQC spectra of the protein dramatically in a manner similar to compound **3**. In addition to

```
NS2B  50 TDMWIERTAD ITWESDAEIT GSSERVDVRL DDDGNFQLMN DPGAPWK GGGGSGGGG
NS3    1 GGVLWDTPSP KEYKKGDTTT GVYRIMTRGL LGSYQAGAGV MVEGVFHTLW HTTKGAALMS
NS3   61 GEGRLDPYWG SVKEDRLCYG GPWKLQHKWN GHDEVQMIVV EPGKNVKNVQ TKPGVFKTPE
NS3  121 GEIGAVTLDY PTGTSGSPIV DKNGDVIGLY GNGVIMPNGS YISAIVQGER MEEPAPAGFE
NS3  181 PEMLRKK
```

Fig. 2. Amino acid sequence of the WNV NS2B–NS3pro constructs used. In addition to the sequence shown, constructs contained the N-terminal sequences MGSSHHHHHHSSGLVPRGSHM (construct 1) or MASMTGHHHHHH (construct 2; Materials and methods). A third construct (construct 3) contained the mutation Lys96^{NS2B} → Ala with N-terminal MASMTGHHHHHH peptide [WNV NS2B–NS3pro(K96A)]. All constructs ended at residue 187 of NS3. Vertical lines identify two autocatalyic cleavage sites [23]. The K96A mutation prevents self-cleavage at either site. Residues without backbone resonance assignments (disregarding proline) are highlighted in orange.

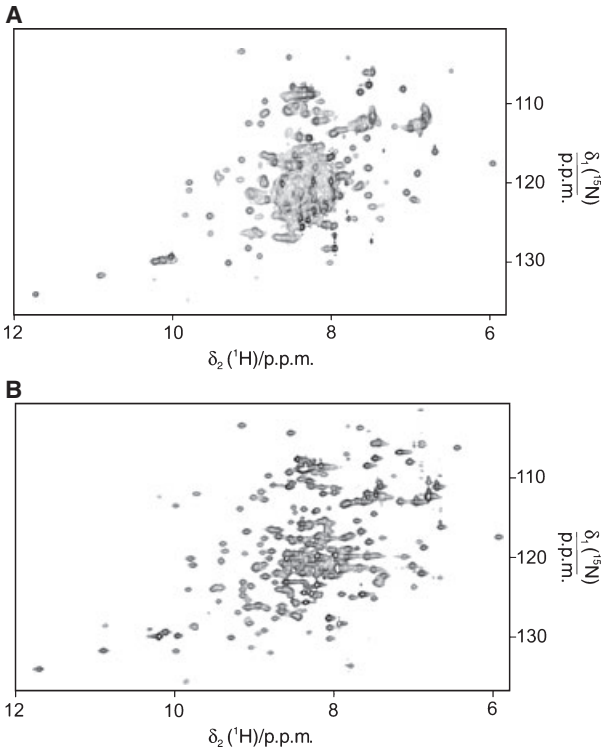

Fig. 3. ^{15}N-HSQC spectra of WNV NS2B–NS3pro(K96A) in the absence and presence of inhibitor **2** at 25 °C. The samples contained 0.9 mM protein in 90% H_2O/10% D_2O containing 20 mM Hepes buffer (pH 7.0) and 2 mM dithiothreitol. The complex with **2** was prepared by adding 15 μL of 100 mM solutions of inhibitor in d_6-dimethylsulfoxide to the protein solution. The spectra were recorded at a ^{1}N NMR frequency of 800 MHz. (A) ^{15}N-HSQC spectrum in the absence of inhibitor. (B) ^{15}N-HSQC spectrum in the presence of compound **2** (3 mM).

improved spectral dispersion, the ^{15}N-HSQC spectra of the complexes with **2** and **3** (Fig. S1) showed marked similarities, indicating that both compounds stabilize the same structure of the enzyme.

Compound **1** originated from the *in vitro* screen (C. Bodenreider *et al.*, manuscript in preparation). It was the first found to improve the NMR spectrum of WNV NS2B–NS3pro in a manner very similar to the inhibitor benzoyl-norleucine-lysine-arginine-arginine-aldehyde (Bz-nKRR-H) [24], which has been used for crystallization [5]. Hence, the first resonance assignments of the protease by 3D NMR spectroscopy were performed using the complex with **1**. Compound **2** was designed to improve the solubility of **1** and lift its two-fold symmetry in order to facilitate the assignment of intermolecular NOEs. **2** bound to WNV NS2B–NS3pro with similar affinity to **1** (IC_{50} of 11 versus 25 μM) (C. Bodenreider *et al.*, manuscript in preparation). Compound **3** inhibited WNV NS2B–NS3 by 35% when tested at 25 μM and had a K_d value of ~40 μM as measured by NMR [10].

Similar to **3** [10], as **1** or **2** were added to the enzyme some of the ^{15}N-HSQC peaks shifted, indicative of chemical shift averaging by chemical exchange on a time scale of tens of milliseconds, whereas others appeared at new positions, as expected for slow exchange in the limit of large chemical shift differences between the free and complexed protein (Fig. S2). The ^{15}N-HSQC spectra did not change significantly when the inhibitors were used in excess.

Resonance assignments

The quality of the ^{15}N-HSQC spectra obtained in the presence of **1**, **2** or **3** was sufficient for sequential resonance assignments using conventional triple-resonance 3D NMR experiments. NMR spectra of NS2B–NS3pro and NS2B–NS3pro(K96A) were closely similar, as expected for a point mutation in a mobile segment of the polypeptide chain. Increased mobility of the segment surrounding residue 96 in NS2B had been suggested by the absence of electron density for the linker peptide between NS2B and NS3 following Asp90 in the crystal structure with BPTI [4] and was confirmed by narrow NMR line shapes.

The resonances of the complex with **1** were assigned using NS2B–NS3pro, whereas the 3D NMR experiments of the complexes with **2** and **3** employed the WNV NS2B–NS3pro(K96A) mutant. The resonance assignments of the complexes with **1** and **3** were supported by combinatorial ^{15}N-labelling (Fig. S3). The assignments of the backbone amide cross-peaks are shown in Fig. S1. Resonance assignments were obtained for the backbone amides of the segments comprising residues 50–96 of NS2B and 17–187 of NS3pro, with the exception of prolines and a few residues with very broad amide peaks. The resonances of the peptide connecting NS2B and NS3pro appeared at chemical shifts characteristic of random coil conformation and were not assigned.

Conformation of WNV NS2B–NS3pro induced by inhibitors

NOEs between NS2B and NS3pro observed for the complex with **2** showed that NS2B docks to NS3pro as in the crystal structures with peptidic inhibitors (Table 1) [4–6]. Furthermore, the similarity of the backbone amide chemical shifts seen in complexes with **1**, **2** and **3** (Fig. S1) indicated that NS2B assumes the same conformation in the presence of any of the three compounds. The crystal structures of NS2B–NS3pro

Table 1. NOEs observed between NS2B and NS3pro in the presence of **2** or **3**.

NS2B	NS3	Distance/Å[a]
Trp53 H^N	Thr27 H^α	3.7
Ala58 H^N	Val22 H^N	3.1
Asp59 H^α	Val22 H^N	3.6
Ser72 H^α	Gly114 H^N	2.8
Arg74 H^α	Val115 H^N	2.6
Val77 H^N	Lys117 H^N	3.3
Gly83 H^N	Lys73 H^α	2.8

[a] Distance in the crystal structure with tetrapeptide inhibitor (2FP7) [5].

in complex with peptide inhibitors or BPTI [4–6] are thus suitable starting points for modelling the complexes with the low molecular mass inhibitors of this study.

Inhibitor binding sites

Because the NMR spectra of the protease complexes with **1** and **2** were very similar, both compounds must bind in the same way. Therefore, we only studied the binding of the nonsymmetric and more soluble compound **2** using intermolecular NOEs. In the 1 : 1 complex with the protease, the proton resonances of the phthalazine ring of **2** were too broad to be observable. (**1** behaved in the same way.) Therefore, we used **2** in an approximately three-fold excess over the protease in order to measure intermolecular NOEs. The maximal solubility of **2** in water was ~3 mM, but aggregation occurred at much lower concentrations. Thus, even at 0.3 mM, the NMR line widths of **2** were broader than expected for a monomeric compound (Fig. S4). Furthermore, negative intramolecular NOEs were observed for a sample at 0.7 mM, indicating an effective molecular mass of > 500 Da. The possibility of self-association made it harder to interpret the intermolecular NOEs observed between the protease and **2**. Consequently, we used the NOE data with **3** to support the assignment of intermolecular NOEs with **2**.

Figure 4 shows intermolecular NOEs observed between WNV NS2B–NS3pro(K96A) and **3**. Although most NOEs could readily be assigned, the difficulty of obtaining complete side-chain resonance assignments for the protein prompted us to seek additional verification that **3** binds to the substrate-binding site of the protease.

In the first experiment, we compared the ^{15}N-HSQC spectra of WNV NS2B–NS3pro(K96A) in the presence of **3** and in the presence of the Bz-nKRR-H inhibitor used in one of the crystal structure determinations [5]. As expected for closely related binding sites, the spec-

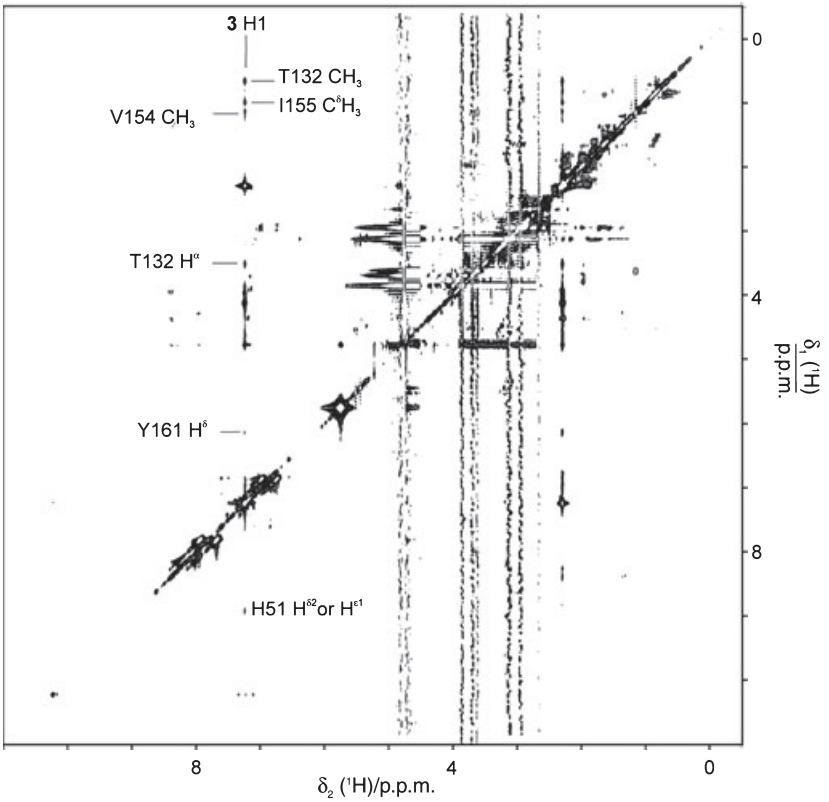

Fig. 4. 2D NOESY spectrum with $^{13}C(\omega_2)/^{15}N(\omega_2)$ half-filter of WNV NS2B–NS3pro(K96A) in complex with **3**. Parameters: 0.9 mM protein and 2 mM **3** in 90% H_2O/10% D_2O containing 20 mM Tris/HCl buffer (pH 7.2) and 2 mM dithiothreitol, 25 °C, mixing time 120 ms, t_{1max} = 34 ms, t_{2max} = 86 ms, 800 MHz ^{1}N NMR frequency. Intermolecular NOEs with the aromatic ring protons of **3** are marked with their assignments. Several of the NOEs are also observed with the methyl groups of **3** at 2.3 p.p.m.

tra were very similar except for chemical shift changes for some of the residues lining the substrate-binding site (Fig. S5).

In another experiment, selectively ^{15}N-Gly-labelled samples of WNV NS2B–NS3pro were prepared of the wild-type protein and the Gly151Ala mutant. Gly151 is located in close proximity to the active-site histidine residue and mutation to alanine should interfere with both enzyme activity and with inhibitors that target the substrate-binding site. Indeed, the G151A mutant was inactive in the enzymatic assay [25] and unable to bind **3** (Fig. S6).

Having established that compound **3** occupies the substrate-binding site, we used the INPHARMA strategy [26] to verify that compound **2** is also residing in the substrate-binding site. A NOESY spectrum of **2** and **3** in the presence of a small quantity of protease revealed an intermolecular cross-peak between the methyl group of **3** and the phthalazine ring of **2**, as expected for an overlapping binding site (Fig. 5).

Table 2 compiles the intermolecular NOEs observed with **2** and **3**. The NOEs with Ile155 were most readily assigned because of their characteristic chemical shifts, whereas other NOEs were assigned using the assumption that the protease fold was that observed in the crystal structures with peptide inhibitors. The fact that all intermolecular NOEs observed with the aromatic ring proton of **3** were also observed with the methyl group was, in most cases, probably a consequence of spin-diffusion. Relaxation during the half-filter delays and the twofold symmetry of **3** further impeded accurate distance measurements.

The data show that both inhibitors are in proximity of Thr132 and Ile155. There are, however, also significant differences between the binding modes of the two compounds. For example, **3** contacts the side chain of His51 in the active site, whereas no equivalent interaction could be found for **2**. No intermolecular NOE with NS2B could be observed because of the difficulty of observing proton resonances of amino and guanidinium groups.

Model building

Docking of compound **2** was performed automatically by DAIM/SEED/FFLD [27–31] using the PDB coordinate set 2FP7 [5], as described previously for **3** [10]. For each compound, a total of 50 poses was kept upon clustering. The pose which best satisfied the intermolecular NOEs (Table 2) was selected as the final model. Not all cross-peaks observed for **2** (Table 2) could be explained as direct NOEs with the protease. This may be because of spin-diffusion during the mixing time of the NOESY experiment, movements of the ligand in the binding pocket or differences in side-chain orientations between the crystal and solution

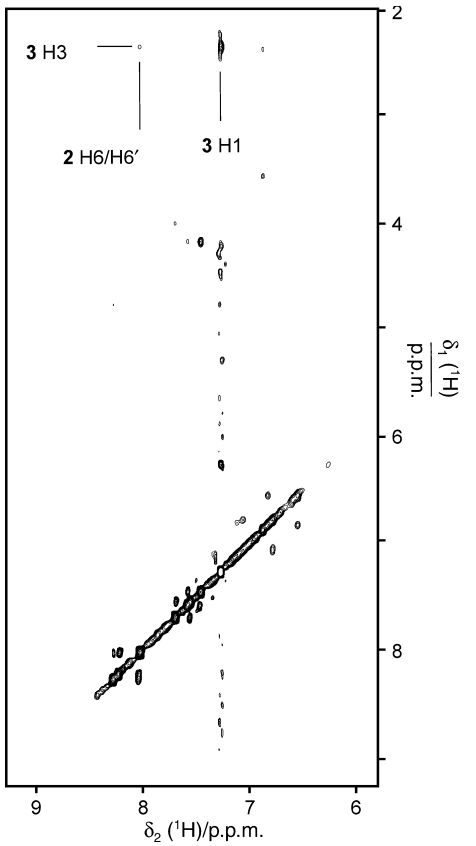

Fig. 5. 2D NOESY spectrum of 0.6 mM **2** and 0.5 mM **3** in the presence of 0.03 mM WNV NS2B–NS3pro(K96A) in D_2O at 25 °C. Under these conditions, the signals of **2** were sufficiently narrow to be observable (Fig. S4C). Other parameters: mixing time 150 ms, t_{1max} = 35 ms, t_{2max} = 71 ms. The cross-peak between **3** H3 and **2** H6 or H6′ is assigned as well as the intramolecular NOE between **3** H3 and H1.

Table 2. Intermolecular NOEs between West Nile virus (WNV) NS2B–NS3pro(K96A) and inhibitors **2** and **3**.

Protons of WNV NS3pro	Compound **2**[a]	Compound **3**
His51 $H^{\delta 2}$		H1 and CH_3
Tyr130 H^{δ}	H6/H6′	
Thr132 $C^{\gamma 2}H_3$	H6/H6′	H1 and CH_3
Thr132 H^{α}		H1 and CH_3
Thr134 $C^{\gamma 2}H_3$	H6/H6′	
Tyr150 H^{δ}	H6/H6′	
Asn152 $C^{\beta}H_2$	H6/H6′	
Gly153 H^{N}	H1	
Val154 $C^{\gamma}H_3$	H1, H2, H5/H5′	H1 and CH_3
Ile155 $C^{\delta 1}H_3$	H1, H2, H3, H4	H1 and CH_3
Tyr161 H^{δ}		H1 and CH_3

[a] NOEs identified in Fig. 6 are underlined.

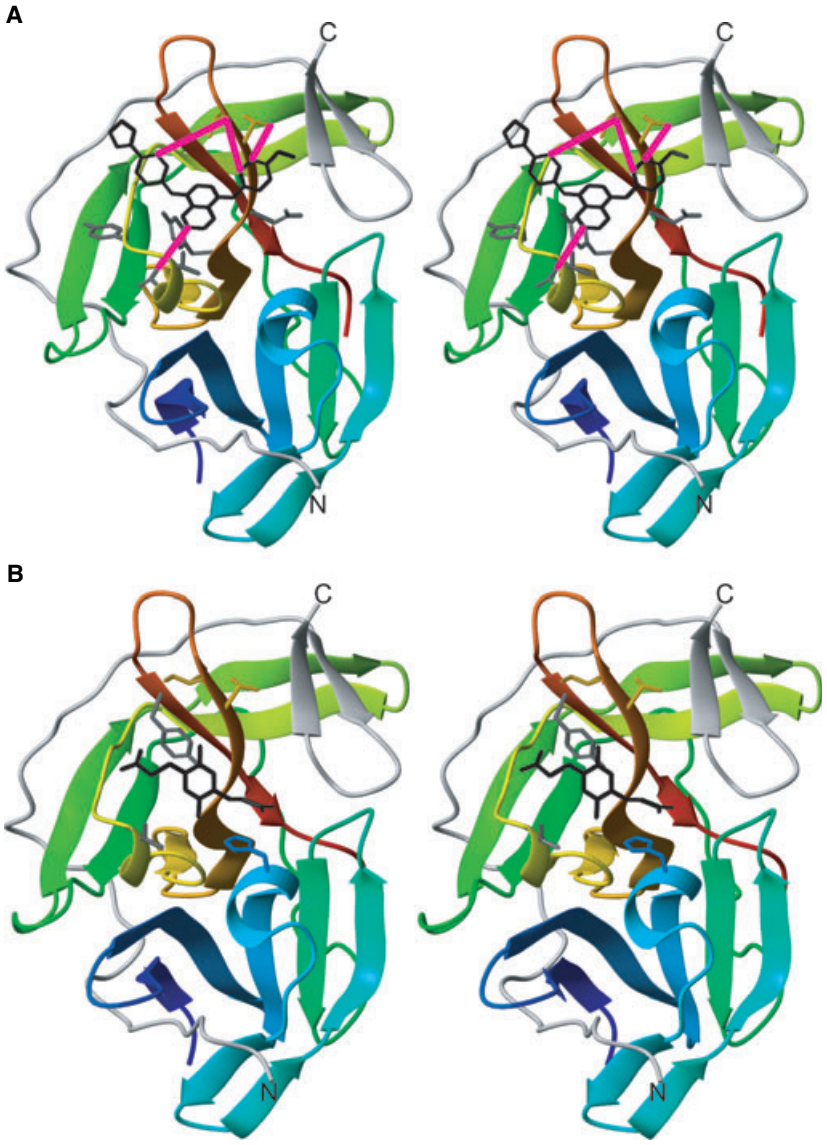

Fig. 6. Stereoviews of models of **2** and **3** bound to WNV NS2B–NS3pro. The protein structure is that by Erbel *et al.* [5], with NS2B drawn as a grey ribbon. Heavy atom representations of **2** and **3** are drawn in black. The side chains of residues for which intermolecular NOEs are reported in Table 2 are shown in a stick representation. (A) Complex with **2**. Selected intermolecular NOEs (Table 2) are highlighted with magenta lines. (B) Complex with **3** reported in Ekonomiuk *et al.* [10].

structure. [For example, the side chain of Ile155 is differently oriented in the structure with BPTI ($\chi_1 = -66°$) [4] than in the structure used for Fig. 6 ($\chi_1 = -180°$) [5], and the intermolecular NOEs observed with Ile155 are in much better agreement with $\chi_1 = -180°$ than $\chi_1 = -66°$.] In the case of aggregation-prone compound **2**, binding of more than a single molecule may have confounded the interpretation of intermolecular NOEs. Nonetheless, the model in Fig. 6A satisfies most NOEs. It places the positively charged cyclic amidine group near the negatively charged side chain of Asp129 which interacts with the positively charged side chain of the P1 residues of Bz-nKRR-H [5] and BPTI [4]. The primary amino group of **2** points towards the C-terminal β-hairpin of NS2B which carries three aspartate residues in a row in positions 80–82. Although **2** belongs to a different class of compounds than **3**, the binding modes of both compounds are not dissimilar (Fig. 6).

Discussion

Competitive inhibition is usually accepted as strong indication that the binding sites of two inhibitors are at least partially overlapping. In the case of the WNV NS2B–NS3 protease, the C-terminal β-hairpin of NS2B is essential for catalytic activity, but has been found far away from the substrate-binding site in the absence of inhibitor [4]. In addition, the substrate-binding site changes significantly between the

structures with and without inhibitor, so that competitive inhibition may conceivably be achieved by binding to a site that prevents NS2B from correct association with the substrate-binding site. In this situation, NMR spectroscopy provides an important tool for the identification of the inhibitor binding site.

No sequence-specific NMR resonance assignments have been reported for the WNV NS2B–NS3 protease. The poor quality of the NMR spectrum of WNV NS2B–NS3pro in the absence of inhibitors is reminiscent of the situation in the homologous NS2B–NS3pro construct from dengue virus type 2, in which selectively $^{15}N/^{13}C$-labelled samples show a great variation in NMR line-width, prohibiting conventional assignment strategies by multidimensional NMR spectroscopy [32]. The dramatic improvement in spectral quality observed upon formation of complexes with our inhibitors is readily explained by a shift in conformational exchange equilibria towards a single conformer. NOEs between NS2B and NS3 indicate that this conformer is related to the conformation observed in the crystal structures of the complex with peptidic inhibitors [4–6], in which the C-terminal β-hairpin of NS2B is positioned near the substrate-binding site rather than far away as in the crystal structure in the absence of inhibitor [4]. We were able to obtain this result without optimized engineering of the NS2B part that had been required to obtain an acceptable NMR spectrum of the closely related dengue virus NS2B–NS3 protease [33].

The NMR data clearly show that the small synthetic inhibitors **1**–**3** bind to the substrate-binding site of WNV NS2B–NS3pro. Competitive inhibition with established peptide inhibitors is thus effected by direct competition rather than by indirect competition via an allosteric inactivation mechanism. Considering the apparent ease with which the C-terminal β-hairpin of NS2B is brought into the vicinity of the active site, our results indicate that the crystal structures of the protease–peptide complexes are valid starting points for the search for low molecular mass inhibitors. Indeed, compound **3** is the first inhibitor of WNV NS2B–NS3pro that has been discovered by a computer search using the crystal structure with a tetrapeptide inhibitor as a template [5,10]. An important implication is that the only available crystal structure of the corresponding dengue virus protease [5] is not a suitable starting point, because it positions the C-terminal β-hairpin of NS2B far from the substrate-binding site.

Although compounds **1**–**3** induce a more uniform structure of WNV NS2B–NS3pro, they are not able to suppress all conformational exchange. For example, we could not assign the backbone amides of Thr132, Gly133 and Gly151 even in the presence of **1**, **2** or **3**, and the backbone resonances of neighbouring residues were broad. All three residues line the substrate-binding pocket. In order to find improved inhibitors, it is thus relevant to explore the conformational space of the protease in a molecular dynamics simulation rather than relying exclusively on the structures observed in the solid state. Intriguingly, the Thr132–Gly133 peptide bond was found to flip spontaneously in the course of two 80-ns and one 40-ns molecular dynamics simulations performed recently [34]. A flip of this peptide bond also presents the main difference in backbone conformation of the substrate-binding site between the crystal structures 2IJO and 2FP7 [4].

The Gly_4–Ser–Gly_4 linker connecting NS2B and NS3pro is highly flexible in solution because the corresponding signals appeared in an intense cluster of peaks at a chemical shift characteristic of a random coil peptide chain. Structural variability of these residues has initially been suggested by the absence of electron density for the linker residues and the C-terminal residues of NS2B following Asn89 in the WNV NS2B–NS3pro(K96A) mutant in complex with BPTI [4]. Also, the recent structure of the protease in complex with a tripeptide inhibitor misses electron density for, respectively, three or all of the residues of the Gly_4–Ser–Gly_4 linker in the two conformers reported [6]. The high mobility observed by NMR for the peptide linker in solution provides a firm explanation for the finding that the covalent linkage between NS2B and NS3 does not restrain the function of the protease [2,9].

In conclusion, compounds **1** and **2** target the substrate-binding site of the WNV NS2B–NS3 protease. Their binding site overlaps with that of compound **3** (Fig. 6). Remarkably, even these small, nonpeptide inhibitors can stabilize the conformation of NS2B observed in crystal structures with peptides. This result provides crucial validation for the use of computational approaches that start from the crystal structures obtained with peptide inhibitors [10]. It also underpins the success of further computations that, by taking into account the conformations sampled by molecular dynamics simulations, led to nonpeptidic lead compounds with low-micromolar affinity [35].

Materials and methods

Materials

Compounds **1** and **2** were synthesized in-house. Compound **3** was obtained from Maybridge (Tintagel, UK) (Cat# S01870SC). Spectra 9 (^{13}C, ^{15}N) media was obtained from Spectra Stable Isotopes (Columbia, MD, USA). $^{15}NH_4Cl$,

$^{13}C/^{15}N$-Silantes (OD2) media, ^{15}N-glycine, $^{13}C/^{15}N$-tyrosine and $^{13}C/^{15}N$-phenylalanine were purchased from Cambridge Isotope Laboratories (Andover, MA, USA). *E. coli* strains Rosetta::λDE3/pRARE and BL21 Star::λDE3 were obtained from Novagen (Gibbstown, NJ, USA) and Invitrogen (Carlsbad, CA, USA), respectively. Synthetic oligonucleotides were purchased from GeneWorks (Hindmarsh, Australia). Sequences of oligonucleotides used are listed in the Supporting Information. *Vent* DNA polymerase and Phusion DNA polymerase were obtained from New England BioLabs (Ipswich, MA, USA). Qiaquick PCR purification and Qiaquick gel extraction kits were purchased from Qiagen (Hilden, Germany).

Preparation of uniformly ^{15}N-labelled WNV NS2B–NS3pro

The *E. coli* strain Rosetta::λDE3/pRARE was transformed with the plasmid pET15b–WNV CF40GlyNS3pro187 (construct 1 of Fig. 2) [5] on Luria–Bertani plates containing 100 μg·mL^{-1} ampicillin and 50 μg·mL^{-1} chloramphenicol. A single transformant colony (~10^8 cells) was diluted with Luria–Bertani media to ~10^7 cells in 1 mL of Luria–Bertani and 100 μL batches of the diluted cells were plated on 15 M9 minimal media plates, containing 5 mM glucose, 0.2% (w/v) glycerol, 100 μg·mL^{-1} ampicillin and 50 μg·mL^{-1} chloramphenicol. Following growth for 2 days at 37 °C, the colonies were collected and resuspended in small volumes of M9 media. Approximately 100 D_{595} units of cells were used to inoculate 500 mL of ^{15}N-autoinduction media containing 0.5 g·L^{-1} $^{15}NH_4Cl$, 100 μg·mL^{-1} ampicillin and 50 μg·mL^{-1} chloramphenicol [16]. Four conical 2-L flasks, each containing 500 mL of ^{15}N-autoinduction cultures, were shaken at room temperature at 200 rpm for 2 days up to an D_{595} value of ~5, yielding ~16.6 g of cells. The cells were suspended in 80 mL of buffer A (50 mM Hepes, pH 7.5, 300 mM NaCl, 5% glycerol, 20 mM imidazole) and lysed by a French press (12 000 psi, two passes). After centrifuging the lysate at 15 000 ***g*** for 1 h, the supernatant was filtered through a 0.45 μm Millipore filter. The filtrate was directly loaded on a 5 mL Ni-NTA column (Amersham Biosciences, Uppsala, Sweden). The bound ^{15}N-WNV NS2B–NS3pro was eluted with an imidazole gradient of 20–500 mM in buffer A. The overall yield of purified protein was 118 mg per 2 L of culture. The protein concentration was determined spectrophotometrically at 280 nm, using a calculated ε_{280} value of 55 760 [36] and the purity checked by SDS/PAGE.

For subsequent testing of different compounds by ^{15}N-HSQC spectra in 3 mm NMR tubes, the protein was subdivided into over 100 batches of 200 μL each, containing 7 mg·mL^{-1} protein in NMR buffer [20 mM Hepes/KOH, pH 6.98, 90% H_2O/10% D_2O, 1 mM tris(2-carboxyethyl)phosphine or 2 mM dithiothreitol]. A sample was prepared for each individual compound by injecting 3 μL of 100 mM solutions of compound in d_6-dimethylsulfoxide into 200 μL of aqueous protein solution in a 3 mm NMR tube.

Preparation of uniformly $^{13}C/^{15}N$-labelled WNV NS2B–NS3pro

$^{13}C/^{15}N$-labelled WNV NS2B–NS3pro was prepared using the same protocol as for ^{15}N-labelled WNV NS2B–NS3pro, except that 2 × 500 mL of $^{13}C/^{15}N$-Silantes media (OD2) were used which were supplemented with 100 μg·mL^{-1} ampicillin and 33 μg·mL^{-1} chloramphenicol. The cells were grown at 37 °C and 200 r.p.m. for 6 h before induction with 0.6 mM isopropyl β-D-thiogalactoside at D_{595} = 0.95. The induced cells were grown at room temperature overnight to D_{595} = 1.1, yielding ~1.8 g of cells which were suspended in 20 mL buffer A for purification as described above. The final yield of $^{13}C/^{15}N$-labelled protease was 9.3 mg in NMR buffer. The sample used for 3D NMR experiments was 0.4 mM in protein in a 5 mm NMR tube.

Preparation of uniformly $^{13}C/^{15}N$-labelled WNV NS2B–NS3pro(K96A)

A $^{13}C/^{15}N$-labelled sample of the K96A mutant of WNV NS2B–NS3pro (construct 3, Fig. 2) was prepared using the same protocol as for $^{13}C/^{15}N$-labelled WNV NS2B–NS3pro, except that 2 × 500 mL of $^{13}C/^{15}N$-Spectra 9 media was used, which was supplemented with 100 μg·mL^{-1} ampicillin and 50 μg·mL^{-1} chloramphenicol. Cells were grown at 37 °C and 200 rpm for 3 h before induction with 0.6 mM isopropyl β-D-thiogalactoside at D_{595} = 1. The induced cells were grown at room temperature overnight to D_{595} = 1.9, yielding ~4.4 g of cells which were suspended in 50 mL buffer A for purification on a 5 mL Ni-NTA column as described above. Following elution from the column, the protein was dialysed against 1 L of 50 mM Tris/HCl (pH 7.6). The dialysate was loaded on a 7.4 mL DEAE-Toyopearl 650M column (2.5 × 1.5 cm; Tosoh Bioscience, Montgomeryville, PA, USA) and the bound protease eluted by a NaCl gradient of 0 mM to 1 M in a buffer of 50 mM Tris/HCl (pH 7.6) and 1 mM dithiothreitol. The final yield of $^{13}C/^{15}N$-labelled protease was 48.4 mg in NMR buffer. NMR samples were 0.9 mM in protein.

Cell-free synthesis of WNV NS2B–NS3pro

Construct 2 (Fig. 2) was designed for optimum expression yields in a cell-free system. Primers 1307 and 1308 (Table S1) were used to amplify the protease gene by PCR from the template plasmid pET15b-WNV CF40glyNS3pro187 using Phusion DNA polymerase. Following digestion by *Nde*I and *Eco*RI, the PCR fragment was transferred into the corresponding site of the pRSET-5b vector [19]. The resulting vector (pRSET-WNV MASMTGH$_6$-

CF40glyNS3pro187) was used for cell-free protein synthesis using a cell extract from *E. coli*.

S30 cell extracts were prepared from the *E. coli* strains Rosetta::λDE3/pRARE and BL21 Star::λDE3 as described previously [17,18,37], including concentration with polyethylene glycol 8000 [38] and heat treatment of the concentrated extracts at 42 °C [39].

Cell-free protein synthesis was performed for 6–7 h either using an autoinduction system with plasmid pKO1166 for *in situ* production of T7 RNA polymerase [40] or using a standard protocol with purified T7 RNA polymerase at 37 or 30 °C [18,21]. The reactions were performed with $\mu g \cdot mL^{-1}$ target plasmid. Site-directed mutants were produced from 5 to 10 $\mu g \cdot mL^{-1}$ PCR-amplified DNA templates. Following cell-free synthesis, the reaction mixtures were clarified by centrifugation (30 000 ***g***, 1 h) at 4 °C.

Cell-free synthesis of combinatorially ^{15}N-labelled WNV NS2B–NS3pro

Five sets of ^{15}N-combinatorially labelled samples [41,42] of construct 2 (Fig. 2) were produced by cell-free protein synthesis. Synthesis was performed using 1 mL reaction mixtures for sets 1–4 and 2 mL for set 5. Set 5 was the only reaction containing ^{15}N-glutamate. This set was prepared using 100 mM potassium succinate in the reaction mixture instead of the usual 208 mM potassium glutamate buffer. Cell-free protein synthesis was performed at 37 °C for 6 h. Following centrifugation, the supernatants were diluted with 5–10 mL of buffer A and the proteins purified by a 1 mL Ni-NTA column (Pharmacia) using a 20–500 mM imidazole gradient in buffer A. The buffer of the samples was exchanged to 20 mM Hepes/KOH (pH 7.0) and 1 mM tris(2-carboxyethyl)phosphine using Millipore Ultra-4 centrifugal filters (molecular mass cutoff 10 000), followed by concentration to a final volume of ~0.2 mL. D_2O was added to a final concentration of 10% (v/v) prior to NMR measurements, resulting in a protein concentration of ~50 μM.

Cell-free synthesis of ^{15}N-Gly labelled wild-type and mutant WNV NS2B–NS3pro

Wild-type and mutant (Gly151Ala) samples of selectively ^{15}N-Gly labelled WNV NS2B–NS3pro (construct 2) were produced by cell-free synthesis from cyclized PCR templates [32] using primers 1314, 1315 and 1131–1134 (Table S1). The synthesis was performed in 1 mL reaction mixtures, using the same conditions and purification protocol as for the combinatorially labelled samples.

NMR measurements

All NMR spectra were recorded at 25 °C using Bruker 800 and 600 MHz Avance NMR spectrometers equipped with TCI cryoprobes. Samples of complexes contained an approximately three-fold excess of inhibitor in order to facilitate the observation of intermolecular NOEs. 3D spectra recorded included HNCA, HN(CO)CA, CC(CO)NH, (H)CCH-TOCSY and NOESY-^{15}N-HSQC (mixing time 60 ms). NOESY spectra with $^{13}C(\omega_2)/^{15}N(\omega_2)$ half-filters (mixing time 120 ms) were used to suppress intramolecular NOEs of the protease and observe intermolecular NOEs. For unambiguous identification of intraligand NOEs, the experiment was also recorded with a ^{13}C-BIRD sequence in the middle of the mixing time which suppressed any NOE from ^{13}C-bound protons of the protein. A 3D ^{13}C-HMQC-NOESY spectrum with $^{13}C/^{15}N(\omega_2)$ half-filter (mixing time 150 ms) facilitated the assignment of the intermolecular NOEs by comparison with the (H)CCH-TOCSY spectrum. The chemical shifts have been deposited in the BioMagResBank (accession number 11053).

Acknowledgements

This work was supported by the Australian Research Council. Docking calculations were performed on the Matterhorn computer cluster at the University of Zürich.

References

1 Hayes EB & Gubler DJ (2006) West Nile virus: epidemiology and clinical features of an emerging epidemic in the United States. *Annu Rev Med* **57**, 181–194.
2 Chappell KJ, Stoermer MJ, Fairlie DP & Young PR (2007) Generation and characterization of proteolytically active and highly stable truncated and full-length recombinant West Nile virus NS3. *Protein Expr Purif* **53**, 87–96.
3 Luo D, Xu T, Hunke C, Gruber G, Vasudevan SG & Lescar J (2008) Crystal structure of the NS3 protease–helicase from Dengue virus. *J Virol* **82**, 173–183.
4 Aleshin AE, Shiryaev SA, Strongin AY & Liddington RC (2007) Structural evidence for regulation and specificity of flaviviral proteases and evolution of the Flaviviridae fold. *Protein Sci* **16**, 795–806.
5 Erbel P, Schiering N, D'Arcy A, Renatus M, Kroemer M, Lim SP, Yin Z, Keller TH, Vasudevan SG & Hommel U (2006) Structural basis for the activation of flaviviral NS3 proteases from dengue and West Nile virus. *Nat Struct Mol Biol* **13**, 372–373.
6 Robin G, Chappell K, Stoermer MJ, Hu S, Young PR, Fairlie DP & Martin JL (2009) Structure of West Nile virus NS3 protease: ligand stabilization of the catalytic conformation. *J Mol Biol* **385**, 1568–1577.
7 Radichev I, Shiryaev SA, Aleshin AE, Ratnikov BI, Smith JW, Liddington RC & Strongin AY (2008) Structure-based mutagenesis identifies important novel deter-

minants of the NS2B cofactor of the West Nile virus two-component NS2B–NS3 proteinase. *J Gen Virol* **89**, 636–641.
8 Chappell KJ, Stoermer MJ, Fairlie DP & Young PR (2008) Mutagenesis of the West Nile virus NS2B cofactor domain reveals two regions essential for protease activity. *J Gen Virol* **89**, 1010–1014.
9 Leung D, Schroder K, White H, Fang NX, Stoermer MJ, Abbenante G, Martin JL, Young PR & Fairlie DP (2001) Activity of recombinant dengue 2 virus NS3 protease in the presence of a truncated NS2B co-factor, small peptide substrates, and inhibitors. *J Biol Chem* **276**, 45762–45771.
10 Ekonomiuk D, Su XC, Ozawa K, Bodenreider C, Lim SP, Yin Z, Keller TH, Beer D, Patel V, Otting G *et al*. (2009) Discovery of a non-peptidic inhibitor of West Nile virus NS3 protease by high-throughput docking. *PLoS Negl Trop Dis* **3**, e356.
11 Mueller NH, Pattabiraman N, Ansarah-Sobrinho C, Viswanathan P, Pierson TC & Padmanabhan R (2008) Identification and biochemical characterization of small molecule inhibitors of West Nile Virus serine protease by a high throughput screen. *Antimicrob Agents Chemother* **52**, 3385–3393.
12 Johnston PA, Phillips J, Shun TY, Shinde S, Lazo JS, Huryn DM, Myers MC, Ratnikov BI, Smith JW, Su Y *et al*. (2007) HTS identifies novel and specific uncompetitive inhibitors of the two-component NS2B–NS3 proteinase of West Nile virus. *Assay Drug Dev Technol* **5**, 737–750.
13 Goodell JR, Puig-Basagoiti F, Forshey BM, Shi PY & Ferguson DM (2006) Identification of compounds with anti-West Nile virus activity. *J Med Chem* **49**, 2127–2137.
14 Gu B, Ouzunov S, Wang L, Mason P, Bourne N, Cuconati A & Block TM (2006) Discovery of small molecule inhibitors of West Nile virus using a high-throughput sub-genomic replicon screen. *Antiviral Res* **70**, 39–50.
15 Noueiry AO, Olivo PD, Slomczynska U, Zhou Y, Buscher B, Geiss B, Engle M, Roth RM, Chung KM, Samuel M *et al*. (2007) Identification of novel small-molecule inhibitors of West Nile virus infection. *J Virol* **81**, 11992–12004.
16 Studier FW (2005) Protein production by auto-induction in high-density shaking cultures. *Protein Expr Purif* **41**, 207–234.
17 Ozawa K, Dixon NE & Otting G (2005) Cell-free synthesis of ^{15}N-labelled proteins for NMR studies. *IUBMB Life* **57**, 615–622.
18 Apponyi M, Ozawa K, Dixon NE & Otting G (2008) Cell-free protein synthesis for analysis by NMR spectroscopy. In *Methods in Molecular Biology, Vol. 426, Structural Proteomics: High-throughput Methods* (Kobe B, Guss M & Huber T, eds), pp. 257–268. Humana Press, Totowa, NJ.
19 Schoepfer R (1993) The pRSET family of T7 promoter expression vectors for *Escherichia coli*. *Gene* **124**, 83–85.
20 Guignard L, Ozawa K, Pursglove SE, Otting G & Dixon NE (2002) NMR analysis of *in vitro*-synthesized proteins without purification: a high-throughput approach. *FEBS Lett* **524**, 159–162.
21 Ozawa K, Headlam MJ, Schaeffer PM, Henderson BR, Dixon NE & Otting G (2004) Optimization of an *Escherichia coli* system for cell-free synthesis of selectively ^{15}N-labelled proteins for rapid analysis by NMR spectroscopy. *Eur J Biochem* **271**, 4084–4093.
22 Shiryaev SA, Ratnikov BI, Chekanov AV, Sikora S, Rozanov DV, Godzik A, Wang J, Smith JW, Huang Z, Lindberg I *et al*. (2006) Cleavage targets and the D-arginine-based inhibitors of the West Nile virus NS3 processing proteinase. *Biochem J* **393**, 503–511.
23 Shiryaev SA, Aleshin AE, Ratnikov BI, Smith JW, Liddington RC & Strongin AY (2007) Expression and purification of a two-component flaviviral proteinase resistant to autocleavage at the NS2B–NS3 junction region. *Protein Expr Purif* **52**, 334–339.
24 Yin Z, Patel SJ, Wang WL, Chan WL, Rao KRR, Wang G, Ngew X, Patel V, Beer D, Knox JE *et al*. (2006) Peptide inhibitors of dengue virus NS3 protease. Part 2: SAR study of tetrapeptide aldehyde inhibitors. *Bioorg Med Chem Lett* **16**, 40–43.
25 Li J, Lim SP, Beer D, Patel V, Wen D, Tumanut C, Tully DC, Williams JA, Jiricek J, Priestle JP *et al*. (2005) Functional profiling of recombinant NS3 proteases from all four serotypes of dengue virus using tetra- and octa-peptide substrate libraries. *J Biol Chem* **280**, 28766–28774.
26 Sánchez-Pedregal VM, Reese M, Meiler J, Blommers MJJ, Griesinger C & Carlomagno T (2005) The INPHARMA method: protein-mediated interligand NOEs for pharmacophore mapping. *Angew Chem Int Ed* **44**, 4172–4175.
27 Kolb P & Caflisch A (2006) Automatic and efficient decomposition of two-dimensional structures of small molecules for fragment-based high-throughput docking. *J Med Chem* **49**, 7384–7392.
28 Majeux N, Scarsi M, Apostolakis J, Ehrhardt C & Caflisch A (1999) Exhaustive docking of molecular fragments on protein binding sites with electrostatic solvation. *Protein Struct Funct Genet* **37**, 88–105.
29 Majeux N, Scarsi M & Caflisch A (2001) Efficient electrostatic solvation model for protein-fragment docking. *Protein Struct Funct Genet* **42**, 256–268.
30 Budin N, Majeux N & Caflisch A (2001) Fragment-based flexible ligand docking by evolutionary optimization. *Biol Chem* **382**, 1365–1372.
31 Cecchini M, Kolb P, Majeux N & Caflisch A (2004) Automated docking of highly flexible ligands by genetic algorithms: a critical assessment. *J Comput Chem* **25**, 412–422.

32 Wu PSC, Ozawa K, Lim SP, Vasudevan SG, Dixon NE & Otting G (2007) Cell-free transcription/translation from PCR amplified DNA for high-throughput NMR studies. *Angew Chem Int Ed* **46**, 3356–3358.
33 Melino S, Fucito S, Campagna A, Wrubl F, Gamarnik A, Cicero DO & Paci M (2006) The active essential CFNS3d protein complex – a new perspective for the structural and kinetic characterization of the NS2B–NS3pro complex of dengue virus. *FEBS J* **273**, 3650–3662.
34 Ekonomiuk D & Caflisch A (2009) Activation of the West Nile virus NS3 protease: molecular dynamics evidence for a conformational selection mechanism. *Protein Sci* **18**, 1003–1011.
35 Ekonomiuk D, Su XC, Ozawa K, Bodenreider C, Lim SP, Otting G, Huang D & Caflisch A (2009) Flaviviral protease inhibitors identified by fragment-based library docking into a structure generated by molecular dynamics. *J Med Chem* (in press).
36 Gill SC & von Hippel PH (1989) Calculation of protein extinction coefficients from amino acid sequence data. *Anal Biochem* **182**, 319–326.
37 Pratt JM (1984) Coupled transcription–translation in prokaryotic cell-free systems. in *Transcription and Translation* (Hames BD & Higgins SJ, eds), pp. 179–209. IRL Press, Oxford.
38 Kigawa T, Yabuki T, Yoshida Y, Tsutsui M, Ito Y, Shibata T & Yokoyama S (1999) Cell-free production and stable-isotope labelling of milligram quantities of proteins. *FEBS Lett* **442**, 15–19.
39 Klammt C, Löhr F, Schäfer B, Haase W, Dötsch V, Rüterjans H, Glaubitz C & Bernhard F (2004) High level cell-free expression and specific labelling of integral membrane proteins. *Eur J Biochem* **271**, 568–580.
40 Ozawa K, Jergic S, Crowther JA, Thompson PR, Wijffels G, Otting G & Dixon NE (2005) Cell-free *in vitro* protein synthesis in an autoinduction system for NMR studies of protein–protein interactions. *J Biomol NMR* **32**, 235–241.
41 Wu PSC, Ozawa K, Jergic S, Su XC, Dixon NE & Otting G (2006) Amino-acid type identification in ^{15}N-HSQC spectra by combinatorial selective ^{15}N-labelling. *J Biomol NMR* **34**, 13–21.
42 Ozawa K, Wu PSC, Dixon NE & Otting G (2006) ^{15}N-labelled proteins by cell-free protein synthesis: strategies for high-throughput NMR studies of proteins and protein–ligand complexes. *FEBS J* **273**, 4154–4159.

Supporting information

The following supplementary material is available:
Fig. S1. Assigned ^{15}N-HSQC spectra of 0.9 mM solutions of ^{15}N-labelled WNV NS2B–NS3pro(K96A) at 25 °C, pH 7.0, in the presence of 3 mM **2** or **3**.
Fig. S2. Selected spectral region from ^{15}N-HSQC spectra showing the effect of increasing concentrations of **2** on the NMR spectrum of WNV NS2B–NS3pro (K96A).
Fig. S3. ^{15}N-HSQC spectra of combinatorially ^{15}N-labelled samples of WNV NS2B–NS3pro in the presence of **1**.
Fig. S4. 800 MHz 1D ^{1}H NMR spectra of the compounds **2** and **3** in the absence and presence of WNV NS2B–NS3pro(K96A) in D_2O solution containing 1.5% d_6-dimethylsulfoxide.
Fig. S5. Superimposition of ^{15}N-HSQC spectra of 0.3 mM WNV NS2B–NS3pro(K96A) in the presence of 0.5 mM **3** or 0.2 mM **3** + 0.4 mM Bz-nKRR-H.
Fig. S6. Superimposition of ^{15}N-HSQC spectra of 0.1 mM solutions of selectively ^{15}N-Gly labelled WNV NS2B–NS3pro(G151A) in the absence and presence of 0.2 mM **3**.
Table S1. PCR primers used in this study to produce different variants of WNV NS2B–NS3pro.

This supplementary material can be found in the online article.

Please note: As a service to our authors and readers, this journal provides supporting information supplied by the authors. Such materials are peer-reviewed and may be re-organized for online delivery, but are not copy-edited or typeset. Technical support issues arising from supporting information (other than missing files) should be addressed to the authors.